Sistematics of Current Disruptions of High Density Tokamak Discharges

G. Lisitano

IPP III/45 Juli 1978

MAX-PLANCK-INSTITUT FÜR PLASMAPHYSIK

8046 GARCHING BEI MÜNCHEN

MAX-PLANCK-INSTITUT FÜR PLASMAPHYSIK

GARCHING BEI MÜNCHEN

Sistematics of Current Disruptions of High Density Tokamak Discharges

G. Lisitano

IPP III/45 Juli 1978

Die nachstehende Arbeit wurde im Rahmen des Vertrages zwischen dem Max-Planck-Institut für Plasmaphysik und der Europäischen Atomgemeinschaft über die Zusammenarbeit auf dem Gebiete der Plasmaphysik durchgeführt.

IPP III/45 G. Lisitano

Sistematics of Current Disruptions of High Density Tokamak Discharges

Abstract

An alternative model of current disruptions is based on resistive displacement of bulk electrons at the plasma boundaries. The model emphasizes that the MHD activity in the plasma interior is dominated by runaways, superthermals and/or the most energetic electrons. The available experimental evidence for this bahavior includes, in particular, schlieren amplitude fluctuations of millimetre waves. The failure of the standard model to explain experimental data and the need for a linking mechanism between plasma-wall interactions and MHD activity in the plasma interior are described first.

1. INTRODUCTION

MHD helical instabilities associated with an excess current density in the hot plasma interior of a tokamak have been described by theories treating internal and major current disruptions /1/. These theories have been taken into account in interpreting observed low-frequency precursor oscillations which have been ascribed to m = 1 and m = 2 MHD tearing modes for respectively precursors of internal and major disruptions /2/,/3/,/4/,/5/. The m = 2 precursors occur when the radial current distribution is such that the q = 2 surface is in the proximity of the limiter. Under these conditions it has been observed that i) the sawtoothing of the internal disruption phase abruptly ceases just before the onset of the exponentially growing precursors and ii) the temperature profile is abnormally flat /6/.

The exponential growth of the m = 2 oscillations has been associated with the existence of magnetic m = 2 islands, which can increase the radial thermal conductivity enough to cool the plasma interior /1/,/7/. Owing to the increasing radial conductivity, a feedback mechanism exists whereby the islands grow to fill a substantial part of the tokamak cross section /7/. By making contact with the limiter the growing islands cause the onset of the current disruption. In addition, a number of effects are suspected of contrib-

uting to the major disruptions. As an example, non-linear coupling between the m = 2 and the weaker m = 1 modes (the latter also being associated with the corresponding m = 1 magnetic island) can lead to large regions of ergodic field lines /1/,/7/. The following arguments show, however, the failure of the above standard model to explain experimental data, and the need for a linking mechanism between plasma-wall interactions and MHD activity in the plasma interior.

2. FAILURE OF THE STANDARD MODEL

The standard interpretation of the m = 0 soft X-ray sawtoothing of the internal disruption phase is that the plasma core is resistively heated until the safety factor drops below unity, causing the m = 1 tearing mode to become unstable, to grow with increasing rate, and ultimately to flatten the electron temperature and safety factor profiles /8/,/9/. In Ref. /9/ the disruptive part of the sawtooth is related to the development of the m = 1 precursors. However, as shown in the upper trace of Fig. 2(b), the m = 1 oscillations are <u>not</u> always superimposed on the soft X-ray sawteeth. There are also discharges which do not even yield coherent, m = 2 external precursor oscillations before the onset of major disruptions. However,

instead of m = 2 oscillations, one invariably observes increasing turbulence in the density fluctuations, indicating strong plasma-wall interaction before the onset of major disruptions. On the other hand it is not clear whether the flattening of the temperature profile is a consequence of the internal m = 1 tearing mode, as is usually claimed. Such a mode, which is associated with the corresponding q = 1 surface, should destroy the confinement of large regions of plasma before the onset of the m = 0 instability. The same applies to the m = 2 modes and q = 2 islands before the onset of major disruptions. Such destruction of confinement, however, is not observed. Furthermore, no experimental proof has been given for the existence of magnetic islands and the connection between the observed oscillations and the internal m = 1 and m = 2 MHD helical instabilities predicted by the theory /1/.

The MHD activity in tokamak plasma is usually interpreted as being dominated by the bulk properties of the electron distribution /9/. This is inferred from electron temperature measurements by Thomson scattering of laser light, before and after internal disruptions. However, these measurements, which are not very sensitive to the most energetic tail of the electron distribution, do not rule out the likelihood that the MHD activity may actually be dominated by the high-energy electrons and/or

superthermals or runaways. In this contest the rapid flattening of the temperature profile at the onset of internal current disruptions may be regarded as due to a rapid redistribution of the most energetic electrons. This hypothesis is supported by the sawtoothing of both soft and hard X-ray emission /3/,/10/, which may be interpreted as due to outward spreading of the most energetic electrons from the center of the plasma. It should be noted here that the assumed sawtoothing symmetry about the q = 1 surface during the internal disruption phase is not experimentally proved. Moreover, the persistent flattening of the current profile which is observed during the precursor oscillations (just after the abrupt cessation of the last sawtooth) may, on the other hand, be interpreted as a progressive failure to replenish superthermal and runaway components, thus supporting the hypothesis of plasma collapse owing to depletion of superthermals or of the most energetic part of the electron distribution. The negative loop-voltage spikes observed in the predisruption and disruption phases may also be regarded as having been generated by a rapid redistribution of runaways, superthermals and/or the energetic tail of the electron distribution, rather than by bulk electrons, as is usually assumed.

It should finally be noted that the asymmetrical tendency of the growing plasma pressure is conducive

to progressive plasma interaction with the outer walls, which is the most likely cause of the observed disruptions. However, relatively little is known about the dynamics of plasma-limiter confinement processes, which should somehow be linked with the observed MHD activity in the plasma interior involving superthermals, runaways and bulk electrons during disruptions. According to the following alternative model, the missing mechanism consists of resistive current displacement of bulk electrons from the gas produced by plasma-wall interaction or gas feed. The model is described by means of a general layout of a few elementary processes which are combined to explain the variety of experimentally observed phenomena. The model has yielded predictions, completely verified, of sawtooth-like emission of hard X-rays from the limiter during internal disruptions /10/, and of flattening of temperature profiles preceding major current disruptions /6/.

According to the model, the evolution of the current disruption is described as:

1) Impurity or gas feed constraint of the bulk electrons.
2) Displacement of the discharge current column.
3) Sifting and spreading of runaway and/or hot electrons.
4) MHD current redistribution.
5) Recovery of runaway and/or hot electrons.

---------Repeat of processes 1 to 5 ---------

6) Unbalanced depletion of runaway and/or hot electrons.

7) Current disruption.

The available experimental evidence of the model include, in particular, a new multibeam schlieren system at λ = 2 mm which permits one to deduce qualitatively the local density redistribution at the onset of and during current disruptions. The discharge current redistribution upon which the model is based is conjectured from the behavior of the local density redistribution.

3. ALTERNATIVE MHD MODEL OF CURRENT DISRUPTIONS

According to the following model, each time the growing off-centered plasma pressure approaches the outer limiter wall, the gas emitted by the plasma-wall interaction produces a layer of high resistivity (3 to 10 times above the pure hydrogen plasma value /11/) which tends to displace the discharge current inwards. Because of the smaller value of the Coulomb collision cross-section of the most energetic electrons in comparison with the Coulomb cross-section of the bulk electrons, the resistive current displacement can only force the latter inwards. This causes, however, destabilization of the discharge current ring owing to the immediate release of that part of the stored magnetic field energy which is associated with the

inward displacement of the current. According to the expression for the self-inductance of the discharge current ring, $L_i = 4\pi R\left[\ln(8R/a) - 1.75\right]$, where a is the minor plasma radius, a smaller value of the major plasma radius R (corresponding to the inward displacement of the bulk-electron current) yields an excess of stored magnetic field energy $dW_m = (1/2)I^2 dL_i$ to be instantaneously depleted.

As will be seen, the release of this excess of field energy determines the flattening of the current profile by increasing the plasma radius, a, of the radial distribution of the most energetic electrons. In fact, assuming infinite conductivity for the current density of the most energetic electrons $J = \sigma E$ (i.e. by neglecting resistive dissipative effects) and by neglecting dissipative radiation effects, the excess of magnetic field energy dW_m can be associated with the behavior of the most energetic electrons by the fundamental MHD energy equation $dW_m/dt + \int v(JxB)dV = 0$, where the first term represents the rate of decrease of the stored magnetic field energy, whilst the second term represents the rate of doing work against the magnetic force JxB. The excess of magnetic field energy to be depleted is therefore that associated with the largest value of the conductivity, which is obviously that related to the most energetic electrons. In other words, the above energy equation represents a "sifting" effect of the MHD

instability which spreads the most energetic electrons outwards from the bulk electrons of the plasma. This partly replaces the inward displacement of the bulk electrons until all runaway or most energetic particles are depleted. The resistive current constriction at the outer plasma edge is therefore partly compensated by the replacement of bulk electrons with the hot electron current carriers which have been displaced outwardly, from the plasma interior, at the onset of the instability. In short, by means of the proposed mechanism the current destabilization in the plasma interior can be excited from the plasma edge by several processes such as, i) interaction of the growing plasma pressure with the outer wall, ii) gas feed, iii) impurity drift waves, etc.. The model is used below to describe the main three phases (internal disruption, predisruption and major disruption) of several discharges. Despite their widely differing appearance, the observed phenomena can be traced back to the systematics of elementary processes mentioned in the introduction.

4. INTERNAL DISRUPTIONS

Sawtooth-like fluctuations of soft X-ray emission /2/,/3/,/12/, are classified in Ref. 2 as internal disruptions. The sawteeth are "inverted", showing a fast rise and a slow drop if one scans a small distance away from the centre of the column.

As already mentioned, each disruption is thought to be caused by precursor oscillations, which have been ascribed in Ref. 2 to the internal m = 1 kink mode /2/, /3/,/4/. According to the proposed model the sawtoothing of the electron density and soft X-rays is interpreted, however, as due to resistive current constraint at the plasma boundaries. Figure 1 shows, for a typical discharge shot in the Pulsator tokamak, the line-integrated phase shift of the λ = 2 mm waves along three vertical radiation chords at a) r = - 2.8 cm, b) r = 0 cm, c) r = + 2.8 cm, for a typical set of discharge parameters, i.e. B_φ = 27 kG, $q(a_L)$ = 3.5, I = 65 kA, $N_e > 10^{14}$ cm^{-3} and pulsed gas inlet at t = 40 ms.

The increasing density at the outer chord in Fig. 1(c) alternately shows a rapid and a slow increment. The rapid increment of the density at the outer chord may be interpreted as the ionization of a gas blast emitted by the interaction of the growing plasma pressure with the outer limiter wall. When the increasing resistivity at the outer plasma edge begins to affect the equilibrium of the current ring, this reacts, as predicted by the proposed model, by spreading the most energetic particles outward, thus flattening their radial distribution. By cooling the plasma edge, i.e. by resistively displacing the bulk-electron current inwards, the gas blast attenuates the plasma-wall interaction, thus allowing the observed sawtooth relaxation of the involved processes until the growing plasma pressure again hits the outer limiter wall.

As shown in Fig. 1(c) for the outer chord, the

pulsed density increment preceding each internal disruption steepens from one instability to the next owing to the increasing strength of the plasma-wall interaction. As shown in Fig. 1(c) by the slow density increments, the growing interaction also increases the relaxation time between two successive rapid increments of density. This behavior levels off in the sawtooth-like density fluctuations of Fig. 1(b) in passing to the central chord. As seen in Fig. 1(a) for the inner radiation chord, the sawtoothing still levels-off inwards into a smoothly slowed-down density increase. All these observations lead to the assumption that the observed sawtoothing is due to a confining process of the plasma-limiter interaction. For a given set of discharge parameters, this is confirmed by the pronounced intensity of molybdenum radiation lines and sawtooth fluctuations for longer and stable discharges /13/.

The outward spreading of the high energy electrons at the onset of each internal disruption is also demonstrated, as predicted by the model, by the "inverted" sawtooth-like modulation of the hard X-rays emitted from the limiter outside /10/,/13/. The inverted sawtoothing of the hard X-rays is shown in the lower trace of Fig. 8. As reported in Ref. /13/, the hard X-ray radiation from the limiter outside is about two order of magnitude larger than that from the limiter inside, which completely support the prediction of the proposed model. As is also predicted by the model, the amplitude of the hard X-ray sawteeth increases with increasing plasma-wall interaction strength until the onset of the major current disruption at t = 94 ms in Fig. 8.

In Fig. 1(c) the noisy behavior of the slow density increment is due to turbulence at the outer plasma edge. Under some conditions, the density and temperature gradients associated with the cooling of the plasma edge may support density drift waves of impurities. According to the proposed model, the resistivity fluctuations associated with the drift waves may excite oscillations of the current distribution, giving rise to the observed m = 1 oscillations on the soft X-ray sawteeth. This does not exlude tearing modes from being present under some discharge conditions. According to the proposed model both oscillations should, however, be considered as an accompanying feature, not as a cause of the instability. This is confirmed by the absence of such oscillations in most discharges. In the following, the feedback mechanism for the exponentially growing precursors preceding the onset of current collapse is described.

5. FEEDBACK MECHANISM OF PRECURSORS

Following the above model, the feedback mechanism for the exponentially growing precursor oscillations is now illustrated on the basis of the typical succession of events given by or deduced from Fig. 2(b). After the last internal disruption at t = 97 ms in Fig. 2(b), upper trace, the sawtoothing of the soft X-rays is strongly attenuated. This indicates that the flattening of the temperature profile at the onset of the last disruption persists

until the onset of the major disruption at t = 100.4 ms. On the other hand, as seen in Fig. 2(b), lower traces, the low-frequency density oscillations start to grow shortly after the onset of the last internal disruption. The exponential growth of these oscillations is accompained by an increased growth rate of the density. As the gas feed is constant, the density increment may be ascribed to impurity gas produced by growing interaction of the plasma with the outer wall. The outward off-centered density increment has been confirmed by simultaneous measurements (not shown here) along an outer radiating chord. Note the systematics of the density increment, in Fig. 2(b), lower traces, accompanying the precursors of major disruption with the corresponding density increment, in Fig. 1(c), accompanying the precursors of minor disruptions.

The density oscillations are well correlated with $\dot{B}_\theta$ low-frequency oscillations (not shown here). These, however, cannot exibit the d.c. perturbation, as the density does, since they are picked up with coils surrounding the discharge current poloidally. Contrary to the magnetic pick-up oscillations, the density exibits a correlation with the sawtoothing of the soft X-ray emission preceding the onset of the growing oscillations. Taking into account the above proposed model, this d.c. perturbation alone can determine the conditions of persistent flattening

of the temperature profile, i.e. through resistive inward displacement of bulk electrons from the outer plasma edge and through the consequent flattening of the radial distribution of the most energetic electrons. The increasing radial conductivity redistributes on its own the O.H. field energy toward the region of plasma-wall interaction, thus determining the feed-back conditions for the growing d.c. instability.

As is well known, the increasing density and temperature gradients at the outer plasma edge support low-frequency drift instabilities through ExB plasma rotation. Therefore, these exponentially growing low-frequency precursor oscillations should be regarded as merely an accompanyng feature of the growing d.c. instability, not a cause of it. There are, in fact, discharges which do not yield coherent low-frequency precursors. Depending on their strength, these density oscillations can also excite, as predicted by the model, corresponding fluctuations in the redistribution of the energetic tail of the electron population in the centre of the plasma. This phenomenon is treated in the standard model as "mode coupling" /3/,/5/,/6/,/7/. The plasma-wall interaction is also demonstrated in Fig. 2(b), upper trace, by the positive pulses of soft X-ray emission just before the major disruption at t = 100.4 ms. These positive pulses, <u>not</u> being associated with enhanced electron temperature, must be due to high-Z impurity emission of soft X-rays.

Precursor oscillations or the precursor density increment do not always lead to the onset of a major disruption. There are discharges where the depletion of the hot component of the electron population leads to a predisruption phase which is characterized by a series of minor disruptions. Besides explosively ejecting energetic particles outwardly, minor and major disruptions are characterized by an inward collapse of the bulk electron current. For the $\lambda = 2$ mm wavelength, used for plasma density measurements, the movement of the bulk electron plasma produces an angular deviation of the exploring millimetre wave rays (schlieren) which provides a qualitative picture of the local density redistribution during minor and major current disruptions.

6. MULTIBEAM SCHLIEREN SYSTEM AT MILLIMETRE WAVELENGTHS

As is well known, the schlieren technique depends on light-ray deviations which are roughly proportional to the transverse electron density gradient. These techniques have hitherto been applied to high density pinch discharges. For the relatively low density values in tokamak plasmas, i.e. $N_e \approx 10^{14}$ cm^{-3}, a finite angular deviation of the exploring ray is encountered in the millimetre wavelength range. The x-component of the total angular deviation of the exploring millimetre wave ray is related to the x-component of the gradient of the refractive index by the expression /14/

$$\Theta_x = \int_0^L \frac{\delta}{\delta x} \ln n(x,y,z)\, dz = \int_0^L \frac{1}{n} \frac{\delta n}{\delta x}\, dz,$$

where n is the refractive index and the integral is taken over the length L of the plasma in the z direction.

In the Pulsator tokamak seven $\lambda = 2$ mm wave beams explore the plasma along vertical chords. The amplitude-independent phase variation of the beam interferometric signals is used to derive the average density distribution of the plasma. All channels are decoupled from each other by interferometric frequency selection. The amplitude decrement ΔA of the deviating beam and the signal amplitude A of the undeviated beam are related to the angular pattern of the radiators used in the Pulsator tokamak by the expression $\Delta A/A = (\Theta_x/\Theta_o)^{1.2}$, where Θ_o is the first zero of the antenna radiation pattern. Combining the above equation with the refractive index $n^2 = 1 - N_e/N_c$, where N_c is the cut-off density corresponding to the $\lambda = 2$ mm wave, we have

$$\frac{\Delta A}{A} \approx \frac{1}{2 N_c \Theta_o} \int_0^L \frac{1}{(1 - N_e/N_c)} \frac{\delta N_e}{\delta x}\, dz.$$

Thus, the electron density gradient may be very sensitively measured by chosing the exploring wavelength for a density cut-off value close to N_e, i.e. $N_e/N_c \leq 1$.

The amplitude variations of the $\lambda = 2$ mm wave beams shown in Figs. 3, 5 and 6 represent the first demonstration of the applicability of schlieren techniques, in the millimetre wave range, to a tokamak plasma.

The amplitude decrement ΔA, representing the refraction losses of the various beams, is most sensitive to density gradients transverse to the radiation path of the waves. Thus, the density variations deduced from the amplitude variations of the millimetre wave beams, which are arranged vertically, are fairly localized in a region about the equatorial plane of the torus, where the most important current redistribution phenomena occur. As shown by the missing data points in the average-density distribution in Fig. 3, the phase information of the wave and hence the density data points, are lost, for $t > 70$ ms, at relatively low values of N_e/N_c of the outer channels owing to a large deviation of the irradiating beams. In spite of this, the schlieren effect allows variations of the local density distribution to be qualitatively detected even for the outer channels.

Assuming a parabolic distribution for N(r):

$$V(r) = V_o\left[1 - \left(\frac{r}{a}\right)^2\right], \quad r < a,$$

where $V_o = N_o/N_c$, N_o is the maximum value of the electron density, and a is the plasma radius, Shmoys /15/ has shown that

$$\theta_x(b) = \sin^{-1} \frac{V_o\left[\left(\frac{b}{a}\right)^2 - \left(\frac{b}{a}\right)^4\right]^{1/2}}{\left[V_o\left(\frac{b}{a}\right)^2 + \left(\frac{1 - V_o}{2}\right)^2\right]^{1/2}}$$

where b is the impact parameter, i.e. the distance of the radiating millimetre wave chord from the centre of

the plasma. Using these calculations, the correspondence between the amplitude variation and the deflection angle of the various beams is shown in Fig. 4(a) and (b) for the density profiles of Fig.3 at t = 40 ms and t = 90 ms respectively, where the density distribution can be resonably assumed as parabolic. Note in Fig. 4(a) the small amplitude variation of the beams, corresponding to the low value of N_e/N_c at t = 40 ms in Fig. 3. In contrast, schlieren effect is clearly seen in Fig. 4(b) to depend on increasing density gradient at the outer millimetre wave channels for the higher value of N_e/N_c at t = 90 ms in Fig. 3.

To interpret the schlieren signals of the seven millimetre wave beams shown in Fig. 3, one should imagine seven light beams irradiating the plasma. However, instead of the usual photografic density, one should relate the amplitude decrement ΔA of the various signals to the usual schlieren photographs. In other words, a decrease of the signal amplitude in Fig. 3 bottom, represents an increase of a fairly localized density gradient in the equatorial plane of the toroidal discharge. The schlieren signals in Fig. 3, bottom, indicate a slightly outwardly off-centered growth of the discharge as seen by the strong signal amplitude decrement of channels 6 and 7 in comparison with the signal decrements of their symmetric channels 2 and 1. The long duration of the shot in Fig. 3 is probably caused by the relatively good

centering of the discharge.

7. PREDISRUPTION

The local density redistribution during current disruptions can be qualitatively deduced from the schlieren signals of the central channel 4 and of the symmetric channels 3 and 5. The schlieren signals are correlated for the shot in Fig. 5 with other discharge parameters such as i) discharge current position signal "OUT-IN", ii) loop voltage U, iii) discharge current I and iv) phase-shift fringes of channels 4 and 5 showing the high density discharge after the pulsed gas inlet at t = 40 ms. In Fig. 5 a predisruption phase takes place during the time interval between the onset of the first negative voltage spike of the loop voltage at t = 78 ms and the onset of the major disruption at t = 90 ms. The predisruption phase is characterized by (from 1 to a few tens of) short pulses of amplitude decrement in the schlieren signal of the central channel 4 and of amplitude increment in the schlieren signal of the internal channel 3. For the shot in Fig. 5 one can observe about ten pulses in the schlieren signal.

A careful study of the schlieren signal of channel 3 in Fig. 5 reveals sawtooth-like behavior of the schlieren amplitude fluctuations in the predisruption phase. The fast rise means a flattening, while the slow drop signifies a steeping local density

profile in a region around the intersection of the equatorial plane of the machine with the channel 3 chord (see Fig. 3). At each sawtooth, the schlieren signal of channel 3 in Fig. 5 shows a gradual, step-like, increase of its amplitude, indicating a corresponding step-by-step inward displacement of the discharge, up to the onset of the major disruption at t = 90 ms, where the whole discharge current collapses by violent impact with the inner discharge wall. Synchronized with the fast rise of the schlieren signals, i.e. with the inward displacement of the density, one can observe in Fig. 5, second trace, negative voltage spikes of the loop voltage. The connection between the fast rise of the schlieren sawtooth signals and the negative voltage spikes reveals that the schlieren signals actually indicate a discharge current redistribution mechanism. In fact, as is well known, the negative voltage spikes originate from a sudden decrement of the self-inductance of the discharge current ring, which, according to the proposed model, is connected with the rapid flattening of the radial distribution of the hot electron population.

The predisruption MHD activity phase supports the pulsed displacement and redistribution of the current without collapsing, i.e. by "apparently" recovering, as will be seen, its initial condition after the rapid displacement. The revelation of this density redistribution in the interior of the plasma

(in spite of the fact that all the phase signals of the seven-channel interferometer system sre strongly impaired by the refraction losses of the λ = 2 mm wave beams) constitutes one of the most useful properties of the schlieren technique. Note in Fig. 5 the correspondence between the inward shift of the plasma, as deduced from the "localized" schlieren signals of channels 3, 4 and 5, and the position signal of the "total" discharge current in the upper trace. The predisruption phase is characterized by an almost constant discharge current, but at each inward displacement, at the leading edge of each schlieren pulse, a small increase of the discharge current is observed. The inverted sawtooth-like current increment is due to the decrement of the self-inductance connected with the step inward displacement of the discharge current ring.

The onset of a predisruption or of a major disruption phase is preceded by bursts of hard X-rays /5/. No hard X-rays are, however, observed for subsequent disruptions /5/, /13/. These observations are in agreement with the proposed model which attribute to a strong plasma-wall interaction the onset of minor or of major disruptions. According to the model, the exponential growth of the precursor plasma-wall interaction lead to the resistive inward displacement of the discharge current. The depletion of the excess magnetic

field energy, associated with the inward displacement of the bulk current, explosively spreads the remaining runaway electrons outwards. Being the runaways completely depleted, the negative voltage spikes of the predisruption phase must then be due to an outwardly spreading of the remaining hot electrons. As is shown in the predisruption phase of another discharge shot in Fig.7, (between t = 82 and t = 100 ms), the redistribution of the hot electron population at each negative voltage spike is demonstrated by the sawtoothing of the soft X-rays, which is similar to that, of smaller amplitude, encountered in the internal disruption phase. Figure 6 shows a predisruption phase with only one predisruption pulse followed, at t = 80 ms, by the onset of the major disruption, which is invariably marked by a rapid increase of the amplitude of the schlieren signal of the inside channel 3. As is confirmed by the current position signal of Fig. 6, upper trace, the rapid increase of the schlieren amplitude of channel 3 corresponds to an inward displacement of the bulk-electron current.

8. CURRENT DISRUPTION

Figure 7 shows, in an enlarged time scale, a disruption phase. In comparison with the last predisruption pulse, the much larger decrement of the self-inductance of the inward collapsing discharge current ring, generates a current pulse which is noticeably larger than those corresponding to the step current displacements of the predisruption phase. The current pulses shown in Fig. 7 may be expressed by $dI/I = -(1/2)dL_i/L_i$, derived from

$dW_m/dt = 0$. The large decrement of L_i and hence the large current pulses of the disruption phase are due to the impact of the cool plasma with the inner wall. The interaction of the collapsing current with the inner wall produces a sudden reduction of the external poloidal magnetic field, giving rise, as shown in Fig. 7, to a positive fast rise of the resistive loop-voltage drop, immediately following each negative voltage spike.

The typical evolution of the current disruption, as indicated by the previous list of processes involved is evident in Fig. 7. Note in Fig. 7 the sawtooth-like behavior of the soft X-rays in the centre of the discharge, during the disruption phase. This and the "inverted" sawtooth behavior of the soft X-rays at the outer plasma shells (shown in Fig. 8 for another discharge shot) are predicted by the proposed model on the basis of the outward displacement and partly recovery of the hot electrons at, respectively, each sudden steep inward and slow outward displacement of the bulk of cool plasma during major current disruptions. At each impact with the inner wall, the collapsing discharge current produces impurity or recycling gas pulses which constrict the discharge current toward the tube axis, thus allowing partial recovery of the thermal population. However, the decreasing discharge current determines a threshold value for the unbalanced inward force of the compensating vertical magnetic field, which excites the intermittent flare-up of the MHD activity until complete extinction of the discharge

is achieved.

9. CONCLUSION

The failure of the standard model to explain experimental data is most evident in the sawtooth relaxation behavior of all three disruption phases (internal, minor and major). Even admitting the existence of the magnetic m = 1 and m = 2 islands in the internal disruption phase, they can hardly enlisted to explain the sawtoothing of the major and minor disruption phases. The alternative MHD model of resistive current displacement satisfies, on the other hand, the unity of the basic behavior for all three disruption phases.

ACKNOWLEDGEMENT

The author is grateful to the Pulsator team for the data of Figs. 7 and 8. For the data of Fig. 2 he is indebted to S. Sesnic for kindly permitting the correlation measurements with his soft X-ray signals and to D.E. Groening, E. Rossetti and N. Gottardi for arranging the enlarged-time-display. The extensive statistical evaluation of many thousands of discharges shot by A. Reiter and E. van Heumen and the skilfull work of E. Rossetti, M. Bergbauer and A. Capitanio are gratefully acknowledged.

References

/1/ KADOMTSEV,B.B., Fiz. Plasmy 1 (1975) 710. [Sov. J. Plasma Phys. 1 (1975) 389]

/2/ von GOELER,S.,STODIEK,W.,SAUTHOFF,N., Phys. Rev. Lett. 33 (1974) 1201.

/3/ T.F.R. GROUP, Nucl. Fusion 17 (1977) 1283.

/4/ MIRNOV,S.V.,EMENOV,I.B., Atomnaya Energiya 30 (1971) 20. [Sov. At. Energy 30 (1971) 14].

/5/ KARGER,F.,LACKNER,G.,FUSSMANN,B.,CANNICI,B.,ENGELHARDT, W.,GENHARDT,J.,GLOCK,E.,GROENING,D.E.,KLÜBER,O., LISITANO,G.,MAYER,H.M.,MEISEL,D.,MORANDI,P.,SESNIC,S., WAGNER,F.,ZEHRFELD,H.P., in Plasma Physics and Controlled Nuclear Research (Proc. 6th. Int. Conf. Berchtesgaden, 1976) IAEA, VIENNA 1 (1977) 267.

/6/ SAUTHOFF,N.,R.,von GOELER,S.,STODIEK,W., Princenton University, Plasma Physics Laboratory, Report PPPL-1379 (1978), (unpublished).

/7/ WHITE,R.B.,MONTICELLO,D.A.,ROSENBLUTH,M.N., Phys. Rev. Lett. 39 (1977) 1618.

/8/ SYKES,A.,WESSON,J.A., Phys. Rev. Lett. 37 (1976) 140.

/9/ JAHNS,G.L.,SOLER,M.,WADDEL,B.V.,CALLEN,J.D.,HICKS, H.R., Nucl. Fusion 18 (1978) 609.

/10/ GLOCK,E., Bull.Am.Phys. 22 (1977) 1201.

/11/ T.F.R. GROUP, Phys. Rev. Lett. 36 (1976) 1306.

/12/ BERLIZOV,A.B.,BOBROVSKIJ,G.A.,BAGDASAROV,A.A.,VASIN, N.L.,VERTIPOROKH,A.N.,VINOGRADOV,V.P.,VINOGRADOVA,N.D., GEGECHKORY,N.M.,GORBUNOV,E.P.,DNESTROVSKIJ,Yu.N., ZAVERYAEV,V.S.,IZVOZCHIKOV,A.B.,LUK'YANOV,S.Yu., LYSENKO,A.B.,NOTKIN,G.E.,PETROV,G.N.,RAZUMOVA,K.A., STRELKOV,V.S.,SHCHEGLOV,D.A., in Plasma Physics and

Controlled Nuclear Fusion Research (Proc. 6th. Int. Conf. Berchtesgaden, 1976) IAEA, VIENNA 1 (1977) 3.

/13/ FUSSMANN,G.,SESNIC,S., Max-Planck-Institut für Plasmaphysik, Report IPP III/37 (1977), (unpublished).

/14/ LEONARD L. STANLEY, in Plasma Diagnostic Techniques (Richard H. Huddlestone and Stanley L. Leonard eds.) p. 46, 47, Academic Press, New York, London (1965).

/15/ SHMOYS,J., J. Appl. Phys. 32 (1961) 689.

Figure Captions

Fig. 1. Sawtooth relaxations of λ = 2 mm wave phase-shift for three vertical radiation chords in Fig. 3 at a) r = - 2.8 cm, b) r = 0 cm, c) r = + 2.8 cm.

Fig. 2 Fringe shift (a) of λ = 2 mm waves (central chord) and correlation measurements (b) of the λ = 2 mm fringe shift (lower traces) with soft X-ray emission (upper trace).

Fig. 3 Average density distribution and schlieren signals (refraction losses) of λ = 2 mm waves for a centered discharge slightly developing towards the outer wall.

Fig. 4 Schlieren amplitude variations and ray path deflections of the λ = 2 mm wave radiating lobes for the shot of Fig. 3, at t = 40 ms and t = 90 ms.

Fig. 5 Schlieren signals (ch. 3, 4 and 5) of a disruptive current instability showing a predisruption phase (between t = 78 ms and t = 90 ms) with sawtooth-like schlieren signal fluctuations (ch. 3). OUT-IN: position signal of the discharge current; U : loop voltage, 2 V per div.; I : discharge current, 20 kA per div.; 8 and 9 : phase fringe-shift of λ = 2 mm waves indicating pulsed gas inlet at t = 40 ms.

Fig. 6 Schlieren signals (ch. 3 and 5) of a major disruptive instability. Note the rapid inward displacemet of the bulk current signalized by the schlieren amplitude variation of ch. 3 at the

onset of the major disruption, at t = 80 ms.

Fig. 7 A discharge current disruption in an enlarged time-scale. Note the sawtooth behavior of i) the soft X-rays of the central emission chord, ii) the discharge current and iii) the position signal for the predisruption phase (between t = 82 ms and t = 100 ms) and the disruption phase (starting at t = 100 ms).

Fig. 8 A discharge shot showing the correlation of the hard X-rays emission with the sawtoothing of the soft X-rays during the internal disruption phase (up to t = 94 ms). Note also i) the increasing amplitude of the hard X-rays signalizing the increasing depletion of runaway electrons and ii) the high amplitude of the sawteeth of the soft X-rays emission at the onset of the major disruption (at t = 94 ms).

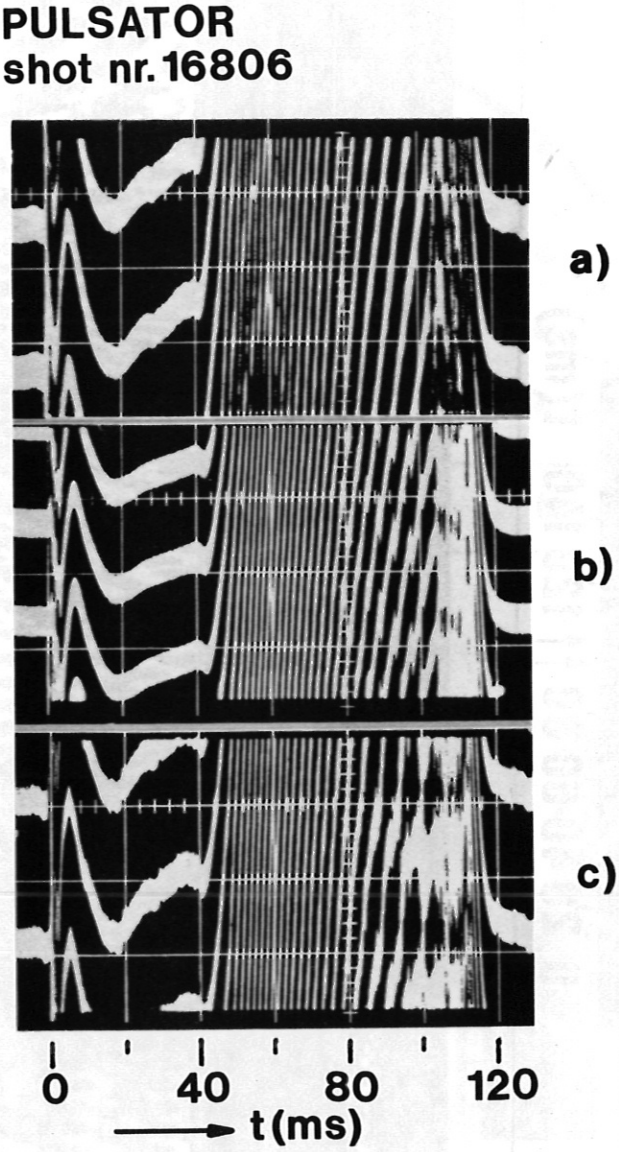

Fig. 1. Sawtooth relaxations of λ = 2 mm wave phase-shift for three vertical radiation chords in Fig. 3 at a) r = - 2.8 cm, b) r = 0 cm, c) r = + 2.8 cm.

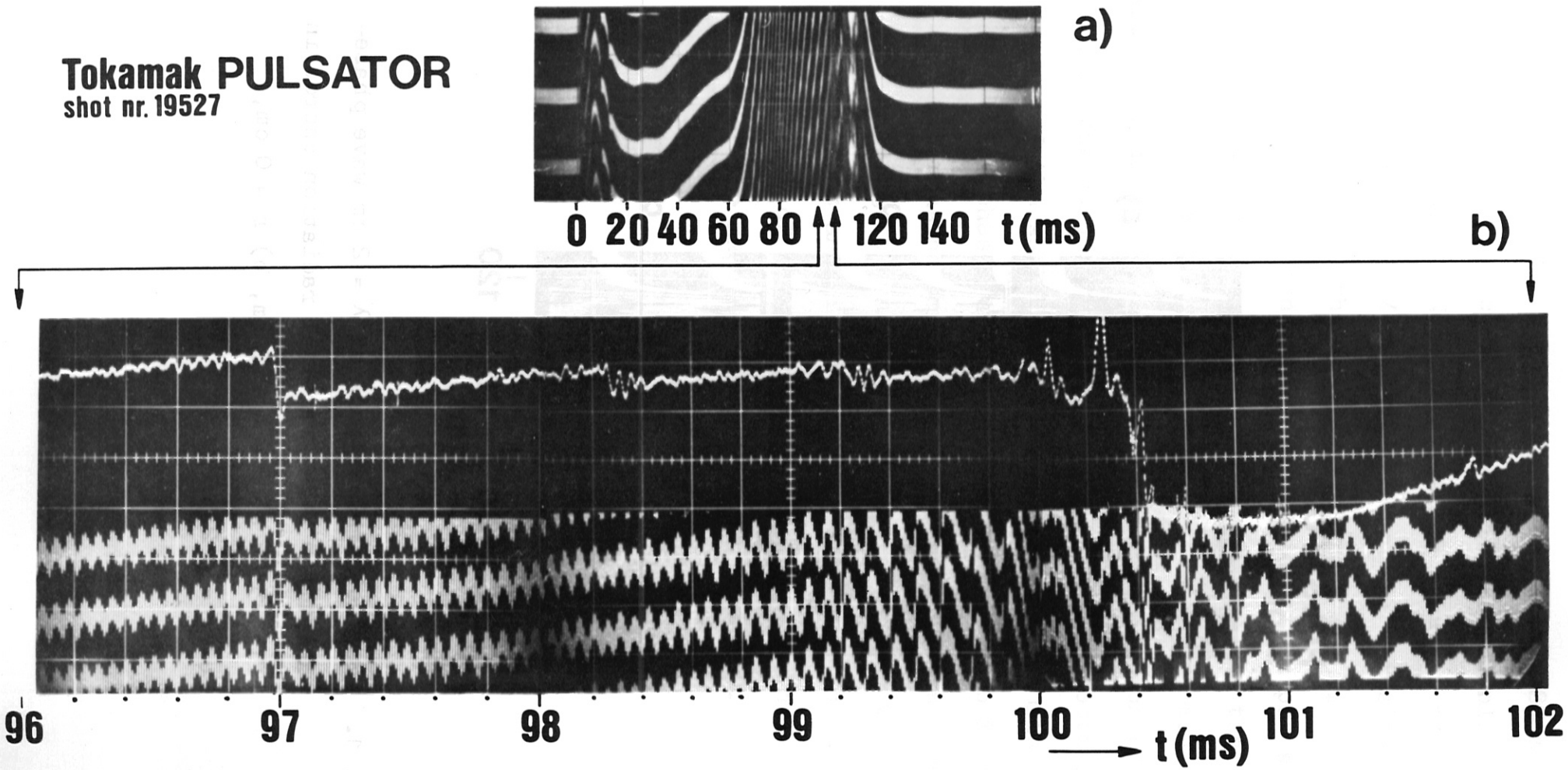

Fig. 2 Fringe shift (a) of λ = 2 mm waves and correlation measurements (b) of the λ= 2 mm fringe shift (lower traces) with soft X-ray emission (upper trace).

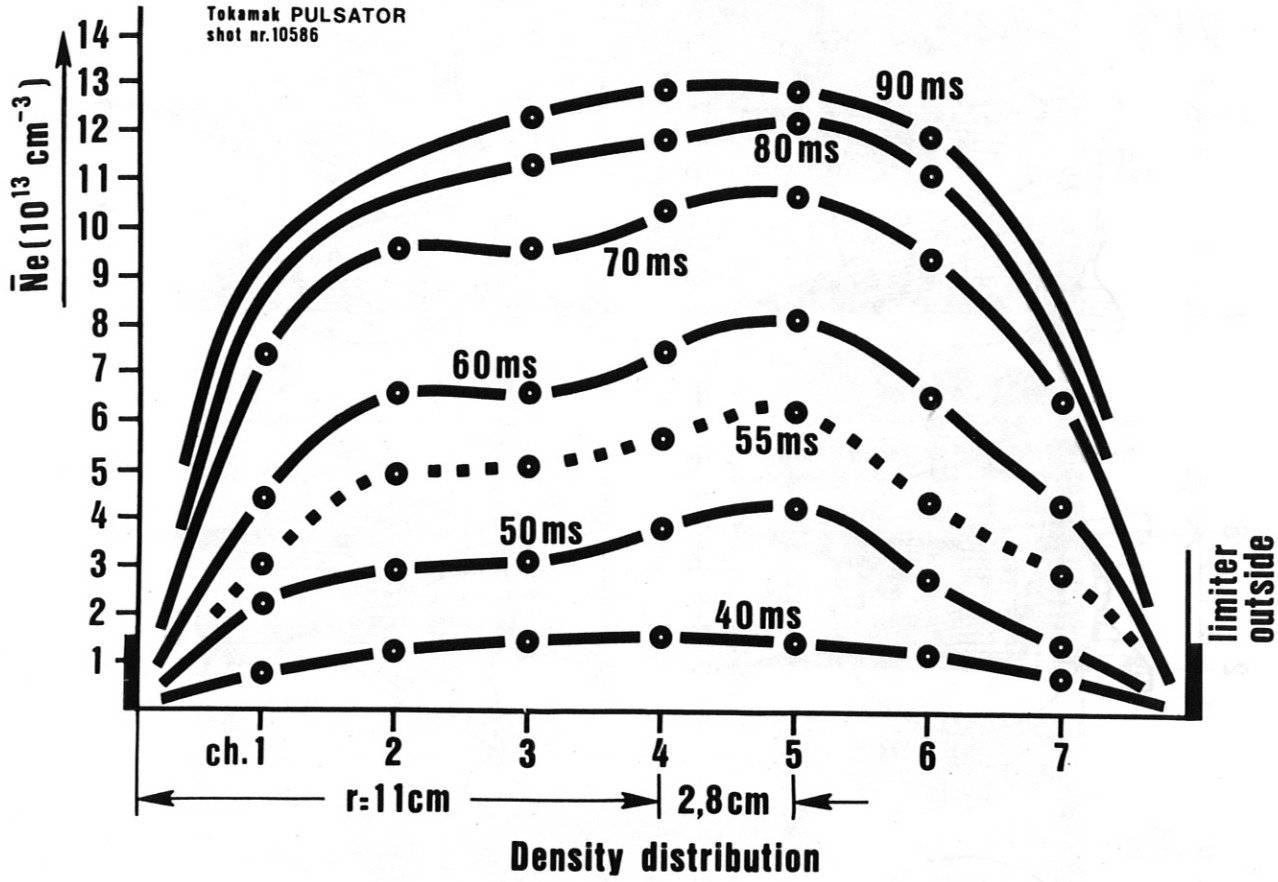

Density distribution

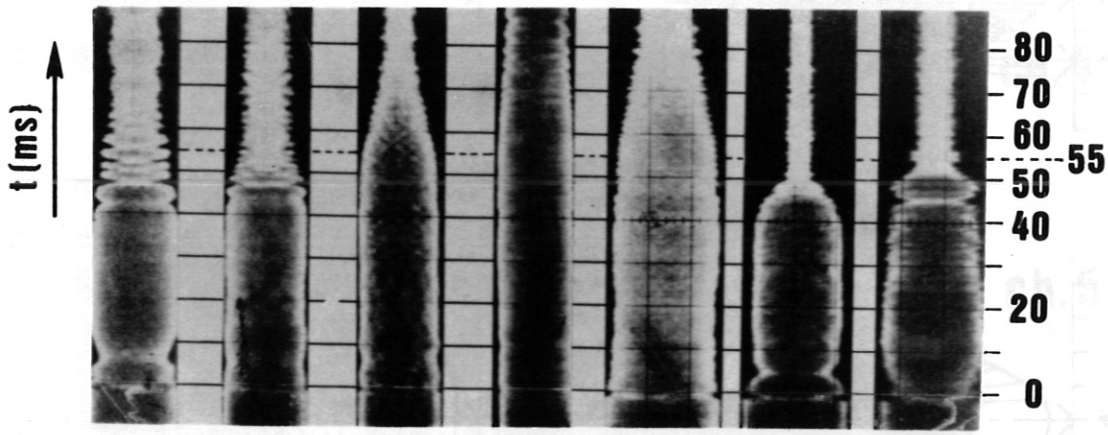

Refraction losses

Fig. 3 Average density distribution and schlieren signals (refraction losses) of $\lambda = 2$ mm waves for a centered discharge slightly developing towards the outer wall.

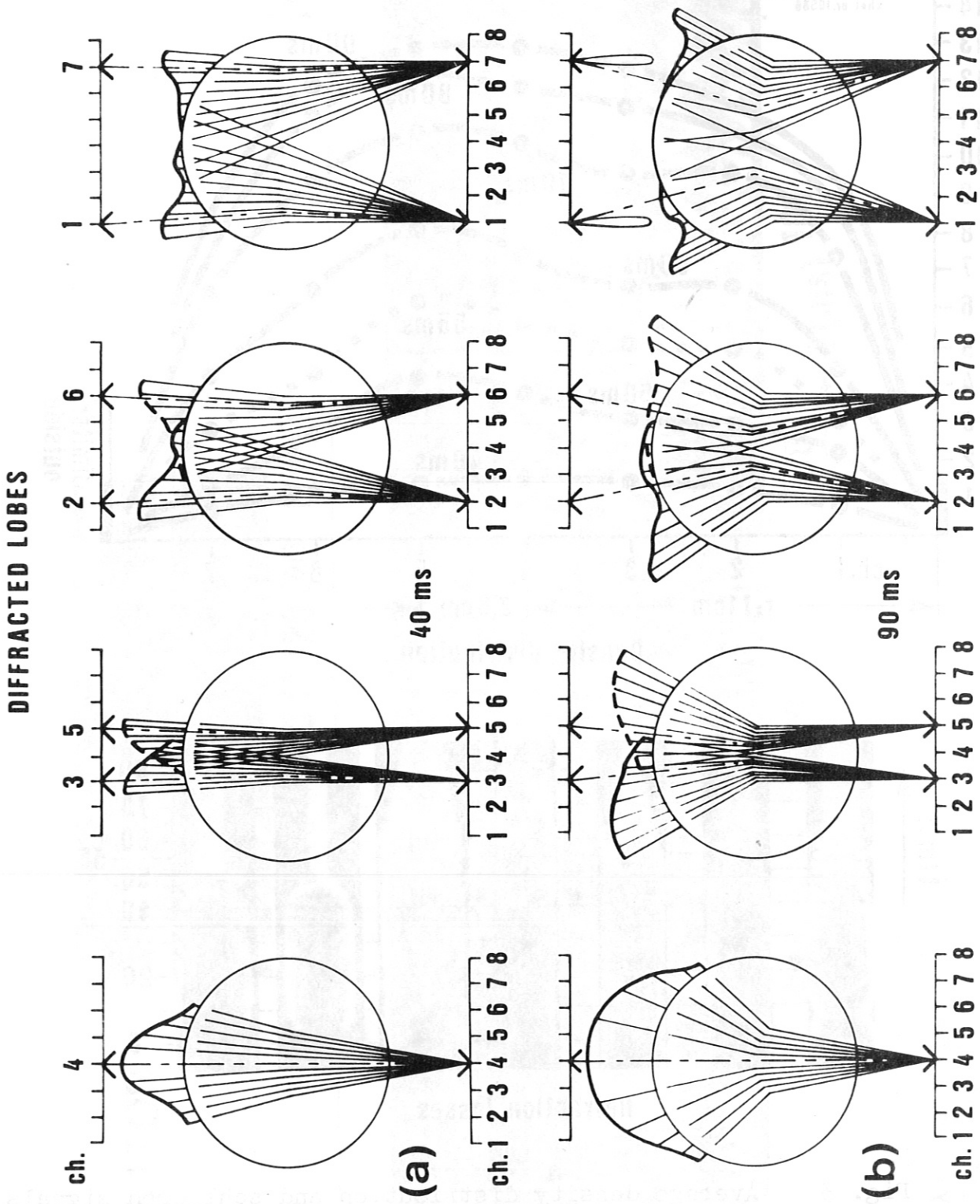

Fig.4 Schlieren amplitude variations and ray path deflection of the λ = 2 mm wave radiating lobes for the shot of Fig. 3, at t = 40 ms and t = 90 ms.

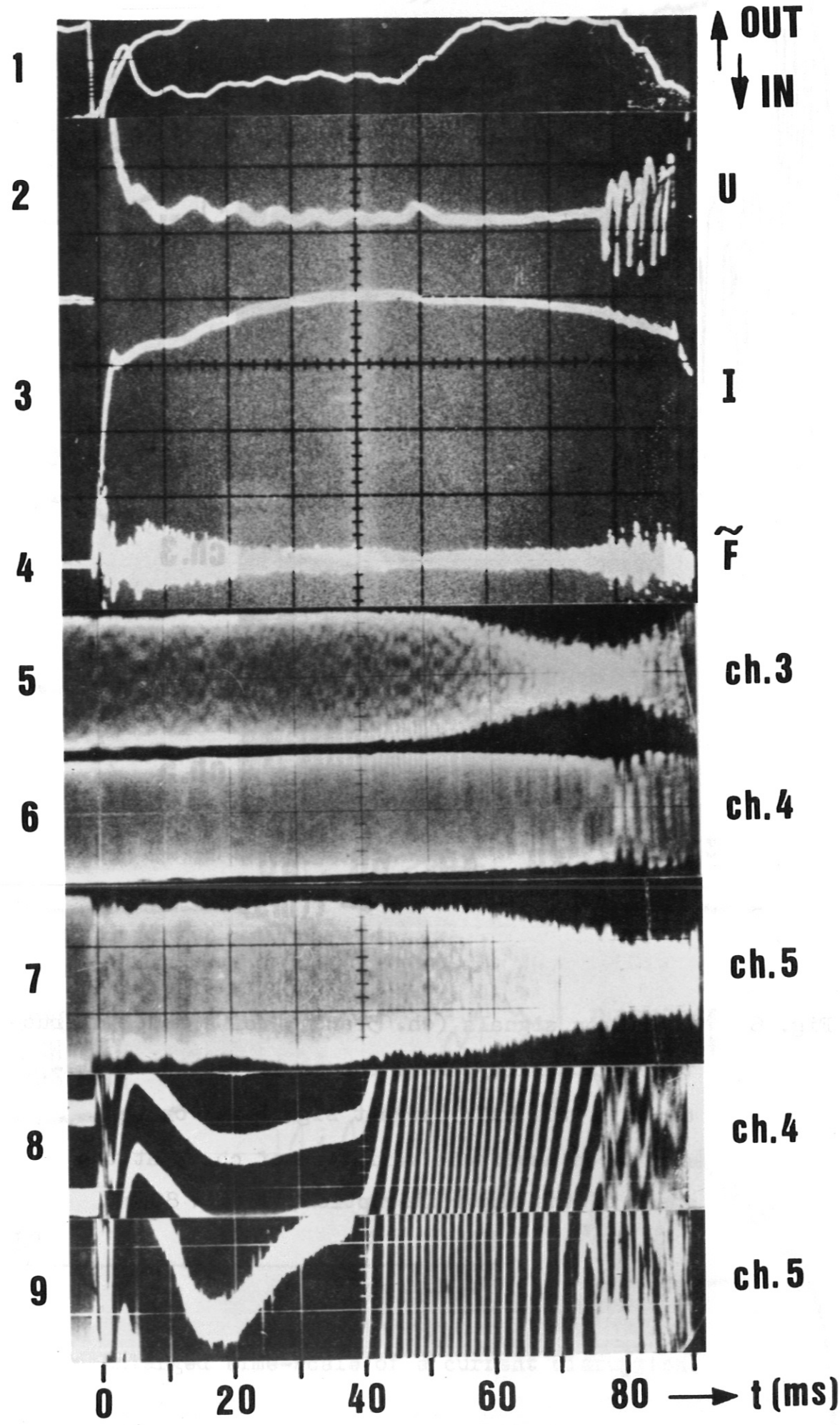

Fig. 5 Schlieren signals (ch. 3, 4 and 5) of a disruption.

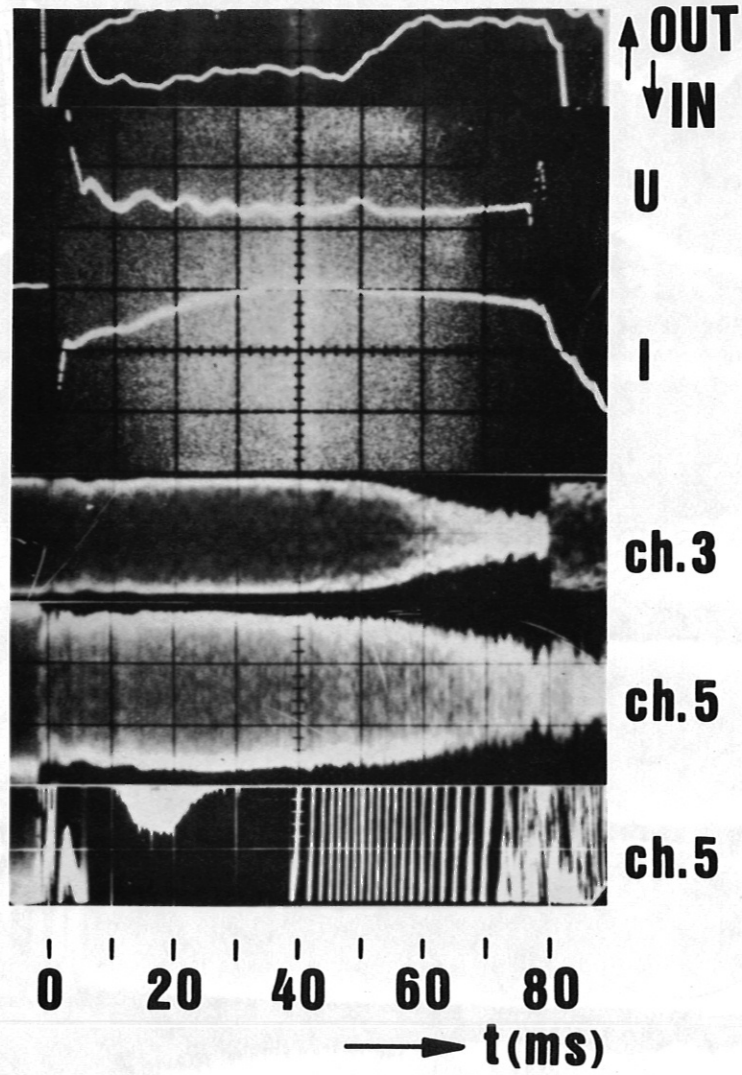

Fig. 6 Schlieren signals (ch. 3 and 5) of a major disruptive instability. Note the rapid inward displacemet of the bulk current signalized by the schlieren amplitude variation of ch. 3 at the onset of the major disruption, at t = 80 ms.

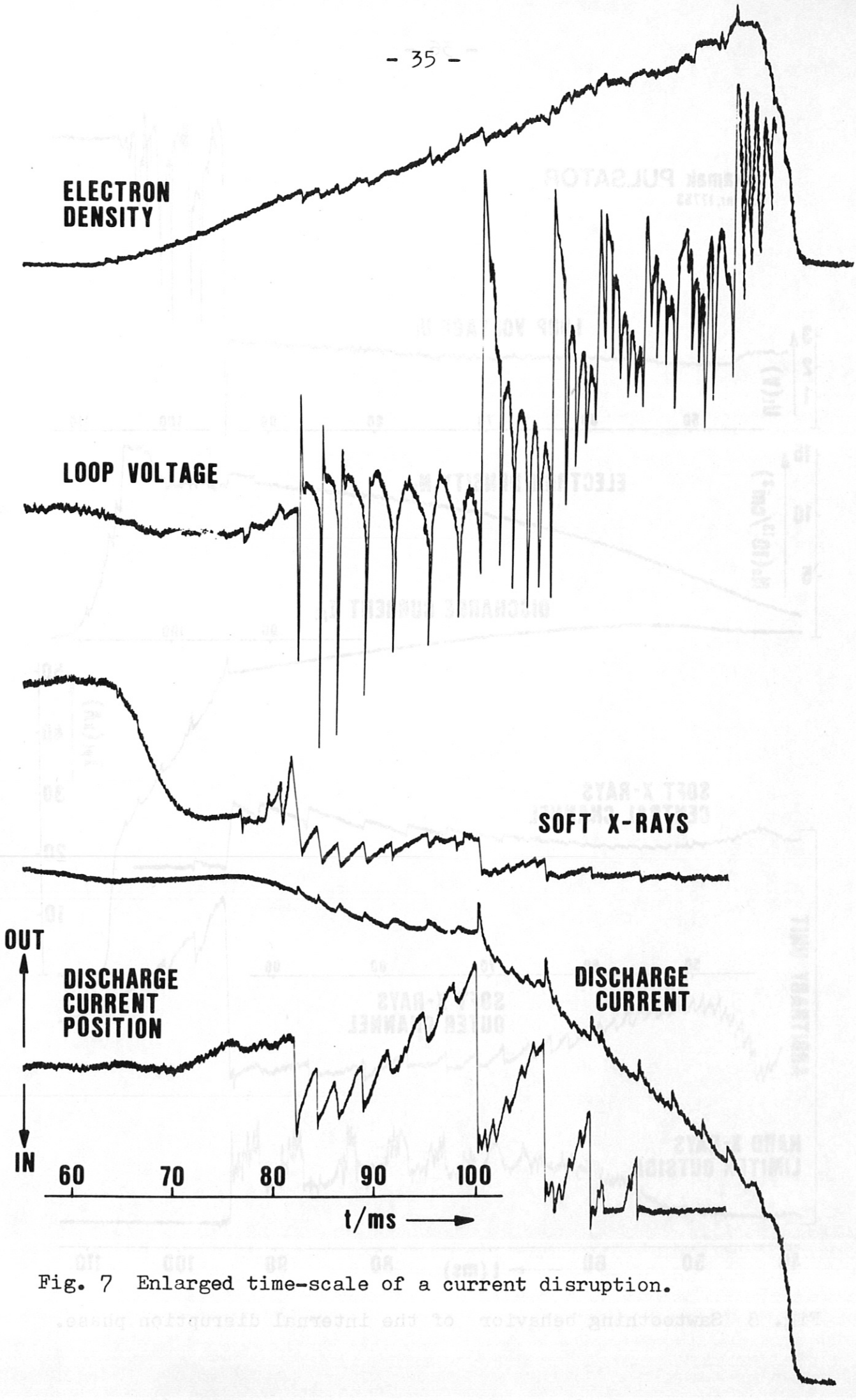

Fig. 7 Enlarged time-scale of a current disruption.

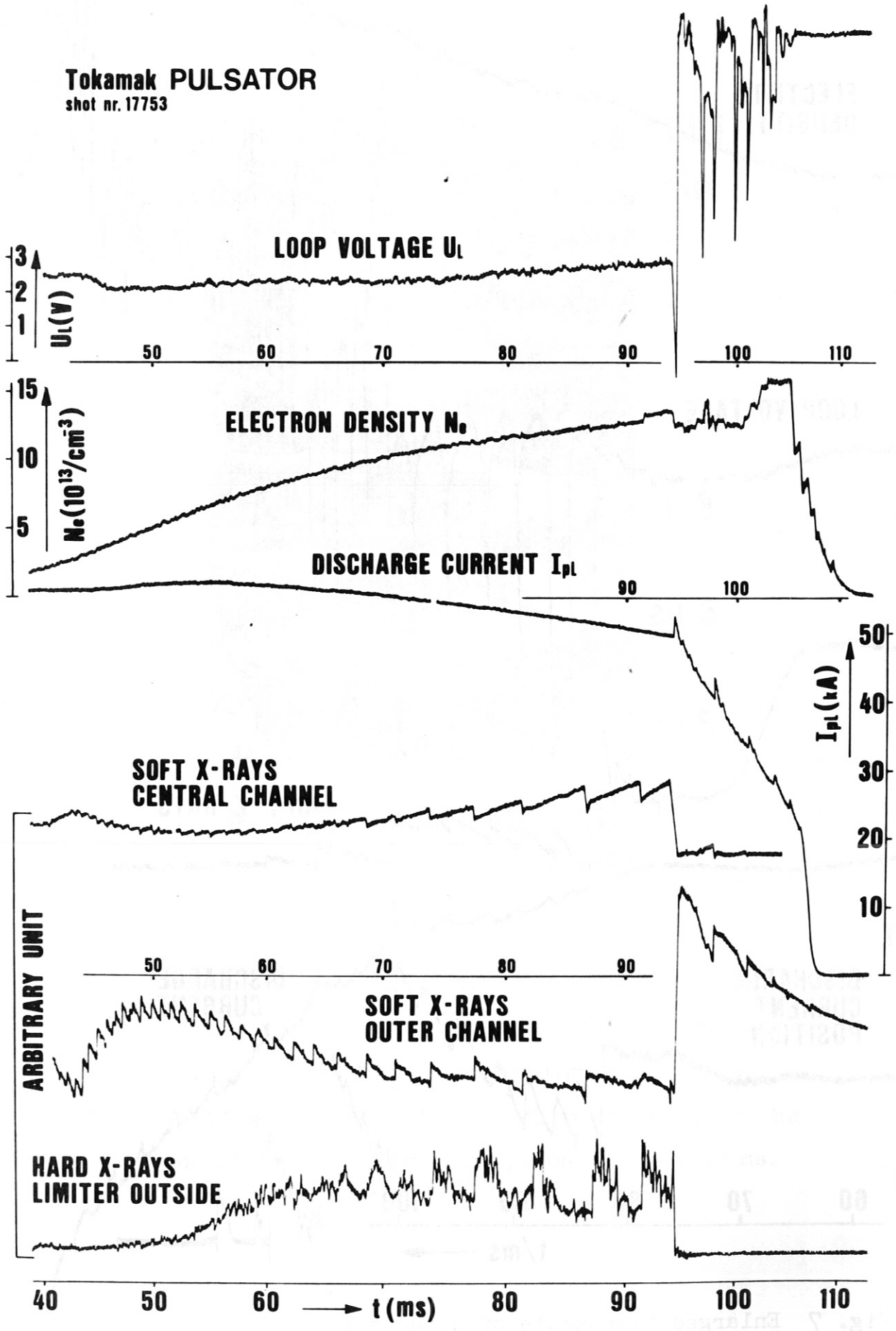

Fig. 8 Sawtoothing behavior of the internal disruption phase.